Available online at www.sciencedirect.com
SCIENCE DIRECT®
Journal of Molecular Catalysis A: Chemical 238 (2005) 241–249
JOURNAL OF MOLECULAR CATALYSIS A: CHEMICAL
www.elsevier.com/locate/molcata

Study of the methane combustion and TPR/TPO properties of Pd/Ce–Zr–M/Al_2O_3 catalysts with M = Mg, Ca, Sr, Ba

Baohua Yue [a], Renxian Zhou [a,*], Yuejuan Wang [b], Xiaoming Zheng [a]

[a] *Institute of Catalysis, Zhejiang University, Hangzhou 310028, PR China*
[b] *Department of Chemistry, Zhejiang Normal University, Jinhua 321004, PR China*

Received 24 February 2005; received in revised form 9 May 2005; accepted 9 May 2005
Available online 5 July 2005

Abstract

The methane combustion behavior is investigated over Pd catalysts supported on Ce–Zr/Al_2O_3 and Ce–Zr–M/Al_2O_3 (M = Mg, Ca, Sr, Ba). Characterization of the catalysts is performed by BET, XRD, TEM, H_2-TPR, O_2-TPO and CH_4/O_2-TPSR techniques. Activity tests in methane combustion show that the addition of trace alkaline earths to Pd/Ce–Zr/Al_2O_3 catalyst obviously increases the catalytic activity of the catalysts under lower reaction temperature conditions, and Pd/Ce–Zr–Ca/Al_2O_3 exhibits the highest catalytic activity and thermal stability among all catalysts. The addition of Ca to Pd/Ce–Zr/Al_2O_3 inhibits the site growth and decomposition of PdO particles and improves the reduction–reoxidation properties of the active PdO species, which increases the catalytic activity and thermal stability of the Pd/Ce–Zr/Al_2O_3 catalyst.

Keywords: Palladium; Ce–Zr/Al_2O_3; Alkaline earths; Thermal stability; Methane combustion

1. Introduction

Catalytic combustion has been demonstrated as one of the most attractive alternatives for performing environmentally friendly combustion of gaseous fuels [1–5]. Recently, this technology has been widely applied in various industrial facilities, such as gas turbine, boiler and incinerator, and so on [6,7]. Since many catalytic processes with environmental application require temperatures of the order 1000–1200 °C, one of the recent requirements for catalyst materials is thermal stability and durability under high temperature conditions, so the major difficulty is to develop a practical catalyst and support that has both high-temperature stability and low-temperature activity [8–11].

Noble metal catalysts are the most active species for performing the complete oxidation of hydrocarbons. Palladium has been reported to be the most active species for the combustion of methane, when operating under oxidizing atmosphere [12,13]. In practice, alumina is usually adopted as support in order to maintain favorable dispersion of active metal to achieve valid utilization of precious metal [14–16]. However, alumina supported palladium catalysts are not stable enough for methane oxidation at the high temperature. For these reasons, addition of a promoter to increase the thermal stability is reported to be an attractive alternative to enhance the performance of conventional catalysts [17–20].

It is well known that ceria is an excellent promoter for noble metal-based combustion catalysts, the role of the ceria being to act as phase-stabilizer for γ-alumina, disperse and stabilize the metal in a more active form, due to a metal–support interaction [21,22]. But with the temperature improvement, especially higher than 1000 °C, CeO_2 readily sinters at elevated temperatures resulting in catalyst deactivation. The addition of Zr and especially the formation of Ce–Zr mixed oxide have been found to be effective in preventing the Ce from sintering. Therefore, the Ce–Zr mixed oxides as additives in alumina supported noble metal catalysts is of great technological importance [10,23].

* Corresponding author. Tel.: +86 571 88273290; fax: +86 571 88273283.
E-mail address: zhourenxian@zju.edu.cn (R. Zhou).

1381-1169/$ – see front matter © 2005 Elsevier B.V. All rights reserved.
doi:10.1016/j.molcata.2005.05.027

Recently we have studied the effect of Ce and Zr modified Pd/Al_2O_3 catalysts for methane combustion. A good thermal stabilization of the alumina is found. A synergism between Ce–Zr and Pd leading to a better activity and thermal stability in the methane combustion is also observed. In order to further improve the catalytic activity and thermal stability, in this paper we investigate the influence of the addition of alkaline earths (Mg, Ca, Sr and Ba) on the methane combustion over $Pd/Ce–Zr/Al_2O_3$ catalyst.

2. Experimental

2.1. Preparation of the catalysts

$Ce–Zr/Al_2O_3$ and $Ce–Zr–M/Al_2O_3$ (M = Mg, Ca, Sr, Ba) supports are prepared by co-impregnation of pseudo-boehmite (S_{BET} = 218 m^2/g) with an aqueous solution of Ce and Zr nitrates, Ce, Zr and alkaline earths (Mg, Ca, Sr, Ba) nitrates, respectively. The samples are dried at 100 °C, and then calcined at 900 °C for 2 h. The total content of Ce and Zr as oxide state ($CeO_2 + ZrO_2$) is 18 wt.%, and the molar ratio of Ce and Zr is 1:4. The content of alkaline earth (M) is 0.4 wt.% for $Ce–Zr–M/Al_2O_3$ supports.

$Pd/Ce–Zr/Al_2O_3$ and $Pd/Ce–Zr–M/Al_2O_3$ (M = Mg, Ca, Sr, Ca) catalysts are prepared by conventional impregnation with an aqueous of H_2PdCl_4 as metal precursors. The impregnated samples are reduced by hydrazine hydrate, filtered and fully washed with deionized water, dried at 100 °C for 12 h and then calcined at 500 °C for 2 h. In order to compare their thermal stability, the catalysts are calcined at 1100 and 1200 °C for 4 h, respectively. The content of Pd for all catalysts is 0.5 wt.%.

2.2. Characterization of the catalysts

2.2.1. BET surface area

The surface areas of $Ce–Zr/Al_2O_3$ and $Ce–Zr–M/Al_2O_3$ (M = Mg, Ca, Sr, Ba) supports and supported Pd catalysts are obtained from N_2 adsorption isotherms (at the liquid nitrogen temperature) with the BET method, using a Coulter OMNISORP-100 apparatus. Prior to adsorption measurements, the samples are degassed under vacuum for 2 h at 200 °C.

2.2.2. X-ray powder diffraction (XRD)

The phase composition of the various samples is determined by means of X-ray powder diffraction (XRD), using a Rigaku D/max-3BX. The operating parameters are: monochromatic Cu Kα radiation, Ni filter, 40 mA, 40 kV, 2θ scanning from 20° to 80°.

2.2.3. Transmission electron microscopy (TEM)

The size of the metallic particles on the supported Pd catalysts is checked with transmission electron microscopy (TEM) using a JEM-2010 (HR) apparatus operated at 200 kV.

2.2.4. Temperature programmed reduction (H_2-TPR) and temperature programmed oxidation (O_2-TPO)

The reduction properties of the supported Pd catalysts are measured by means of H_2-TPR. Prior to experiments, 50 mg of the catalysts are pre-treated in air at 300 °C for 0.5 h before the TPR. The reduction gas is 5 vol.% H_2 in N_2, which is purified with deoxidizer and silica gel. The reaction temperature is programmed to rise at a constant rate of 10 °C/min and the flow-rate is 40 ml/min. Amount of H_2 consumption during the H_2-TPR is measured by a thermal conductivity detector (TCD), and the effluent H_2O formed during H_2-TPR is adsorbed with a 5 A molecular sieve.

The reoxidation properties of the reduced catalysts are measured by means of O_2-TPO. An 100 mg of the catalysts is used, and pre-reduced in H_2 atmosphere at 500 °C for 1h before the TPO experiments, and then cooled to room temperature. The oxidation gas is 5 vol.% O_2 in He. TPO experiments are carried out with a flow rate of 40 ml/min, increasing the temperature from room temperature to 1000 °C at a heating rate of 20 °C/min, and then decreasing the temperature from 1000 to 300 °C at a cold rate of 20 °C/min. Amount of O_2 consumption during the O_2-TPO is also measured by a thermal conductivity detector (TCD).

2.2.5. Temperature programmed surface reaction (CH_4/O_2-TPSR)

The temperature programmed surface reaction (TPSR) is carried out in the same apparatus as the catalytic activity tests analysis. The feed composition is 0.5 vol.% methane, 2 vol.% oxygen and balance of nitrogen, and the space velocity is 72 000 h^{-1}. The reaction temperature during the CH_4/O_2-TPSR is increased from room temperature to 1000 °C at a heating rate of 20 °C/min and decreased from 1000 to 300 °C at a cold rate of 20 °C/min.

2.3. Tests of catalytic activity for methane combustion

Catalytic activity tests for methane combustion are carried out using a conventional microreactor (i.d. 8 mm) under atmospheric pressure. The powdered catalysts are sieved (40–60 mesh) and packed between the layers of quartz wool. A gas mixture of 1.5 vol.% methane and 6.0 vol.% oxygen in nitrogen is passed over the catalysts at a space velocity of 18 000 h^{-1}. The analyses of the reactor effluent are performed by on-line gas chromatography.

3. Results and discussion

3.1. BET surface area

Table 1 lists the BET surface areas of Al_2O_3, $Ce–Zr/Al_2O_3$ and $Ce–Zr–M/Al_2O_3$ (with M = Mg, Ca, Sr, Ba) supports calcined at 900 °C and supported Pd catalysts calcined at 1100 °C, respectively. From Table 1, it can be seen that after calcinations at 900 °C, the addition of cerium and zirconium

Table 1
Surface area of the supports and supported Pd catalysts

Supports	S_{BET} calcined at 900 °C (m^2/g)	Catalysts	S_{BET} calcined at 1100 °C (m^2/g)
Al_2O_3	98	Pd/Al_2O_3	25
$Ce–Zr/Al_2O_3$	106	$Pd/Ce–Zr/Al_2O_3$	49
$Ce–Zr–Mg/Al_2O_3$	111	$Pd/Ce–Zr–Mg/Al_2O_3$	52
$Ce–Zr–Ca/Al_2O_3$	112	$Pd/Ce–Zr–Ca/Al_2O_3$	54
$Ce–Zr–Sr/Al_2O_3$	116	$Pd/Ce–Zr–Sr/Al_2O_3$	60
$Ce–Zr–Ba/Al_2O_3$	118	$Pd/Ce–Zr–Ba/Al_2O_3$	63

oxides to alumina results in an enhanced thermal stability of the supports, which maintains large surface area. The measurements of the BET surface area of the stabilized alumina reflect the significant influence of Ce and Zr up to 1100 °C. The surface area of the non-doped Pd/Al_2O_3 undergoes a sharp decrease after calcinations at 1100 °C due to sintering, showing a specific surface area of only 25 m^2/g. In contrast, the sample containing Ce and Zr exhibits surface areas of 49 m^2/g after equivalent thermal treatment. In addition, the addition of alkaline earths can further improve the thermal stability of the $Pd/Ce–Zr/Al_2O_3$ support.

3.2. XRD

The XRD patterns of $Pd/Ce–Zr/Al_2O_3$ and $Pd/Ce–Zr–M/Al_2O_3$ catalysts calcined at 900 and 1100 °C are shown in Figs. 1 and 2, respectively. From Fig. 1, it can be seen that there are no obvious peaks corresponding to Pd or PdO crystal phase due to too low palladium loading for all the catalysts. All the supports exhibit almost similar XRD patterns after calcined at 900 °C. The tetragonal and cubic phases of $Ce_xZr_{1-x}O_2$ solid solution are observed in all the samples. The supported $Ce_xZr_{1-x}O_2$ solid solution shows mainly the tetragonal phase due to high Zr loading, and the crystalline structure of alumina remains γ-alumina phase. From Fig. 2, it can be seen that after calcined at 1100 °C, the peaks of the $Ce_xZr_{1-x}O_2$ solid solution become sharper and more intense, corresponding to an increase in size of the crystalline particle. But it is interesting to note that the crystalline structure of alumina does not convert to α-alumina phase, which is typical for this temperature. The results show that the presence of Ce–Zr or Ce–Zr–M obviously improves the thermal stability of the alumina. No $CeAlO_3$ phase is found in the samples calcined at 1100 °C, which implies that the presence of zirconia can prevent CeO_2 from interacting with Al_2O_3.

3.3. Catalytic activity of methane combustion

Fig. 3 shows the light-off curves of methane combustion over $Pd/Ce–Zr/Al_2O_3$ and $Pd/Ce–Zr–M/Al_2O_3$ catalysts calcined at 500 °C. From Fig. 3, it can be seen that the addition of trace alkaline earths obviously improves the activity of $Pd/Ce–Zr/Al_2O_3$ catalyst for methane combustion under lower reaction temperature conditions, and $Pd/Ce–Zr–Ca/Al_2O_3$ exhibits the highest catalytic activity among all catalysts. The temperature for the 20% conversion ($T_{20\%}$) of decreases in the order: $Pd/Ce–Zr/Al_2O_3$ (345 °C) > $Pd/Ce–Zr–Ba/Al_2O_3$, $Pd/Ce–Zr–Sr/Al_2O_3$ (320 °C) > $Pd/Ce–Zr–Mg/Al_2O_3$, Pd/

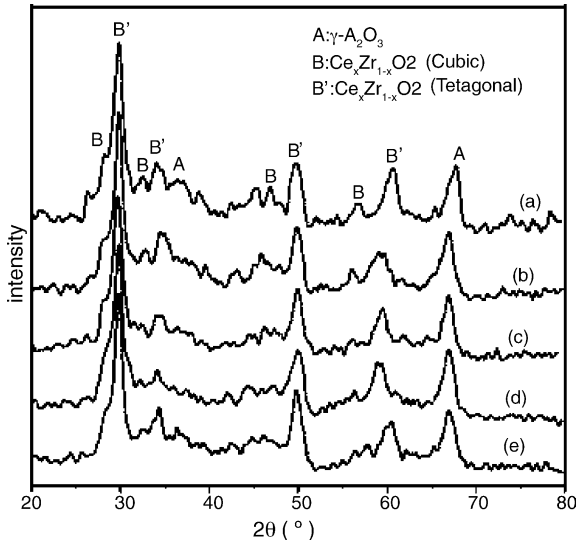

Fig. 1. XRD patterns of the catalysts calcined at 500 °C: (a) $Pd/Ce–Zr/Al_2O_3$; (b) $Pd/Ce–Zr–Mg/Al_2O_3$; (c) $Pd/Ce–Zr–Ca/Al_2O_3$; (d) $Pd/Ce–Zr–Sr/Al_2O_3$; (e) $Pd/Ce–Zr–Ba/Al_2O_3$.

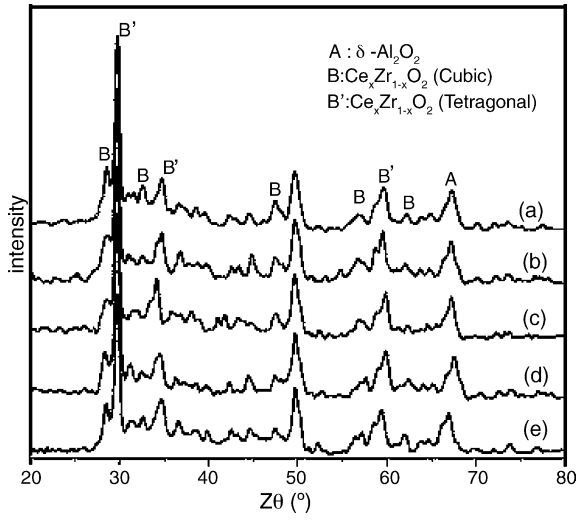

Fig. 2. XRD patterns of the catalysts calcined at 1100 °C: (a) $Pd/Ce–Zr/Al_2O_3$; (b) $Pd/Ce–Zr–Mg/Al_2O_3$; (c) $Pd/Ce–Zr–Ca/Al_2O_3$; (d) $Pd/Ce–Zr–Sr/Al_2O_3$; (e) $Pd/Ce–Zr–Ba/Al_2O_3$.

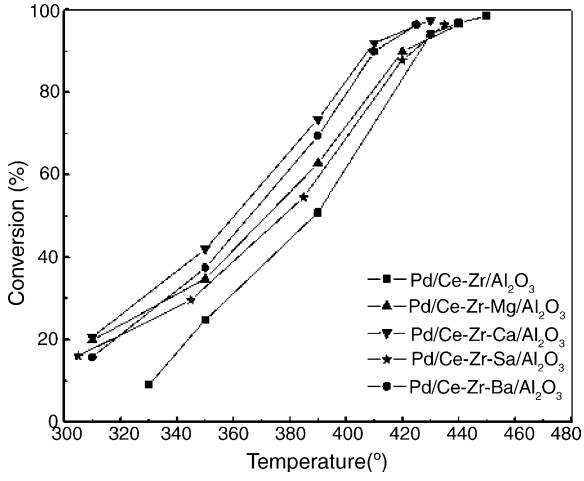

Fig. 3. Light-off curves of methane oxidation over Pd/Ce–Zr/Al_2O_3 and Pd/Ce–Zr–M/Al_2O_3 (M = Mg, Ca, Sr, Ba) catalysts calcined at 500 °C.

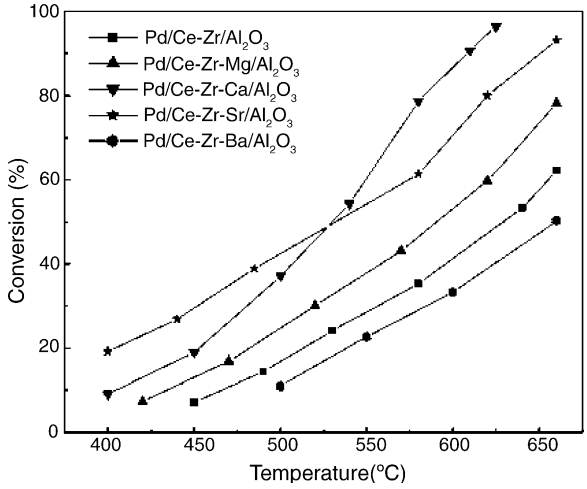

Fig. 5. Light-off curves of methane oxidation over Pd/Ce–Zr/Al_2O_3 and Pd/Ce–Zr–M/Al_2O_3 (M = Mg, Ca, Sr, Ba) catalysts calcined at 1200 °C.

Ce–Zr–Ca/Al_2O_3 (310 °C). The temperature for the 90% conversion ($T_{90\%}$) decreases in the order: Pd/Ce–Zr/Al_2O_3 (430 °C) > Pd/Ce–Zr–Sr/Al_2O_3 (425 °C) > Pd/Ce–Zr–Mg/Al_2O_3 (420 °C) > Pd/Ce–Zr–Ba/Al_2O_3 (410 °C) > Pd/Ce–Zr–Ca/Al_2O_3 (405 °C).

Fig. 4 shows the light-off curves of methane combustion over Pd/Ce–Zr/Al_2O_3 and Pd/Ce–Zr–M/Al_2O_3 catalysts calcined at 1100 °C. From Fig. 4, it can be seen that the activity for methane combustion slightly decreases for all the catalysts after calcined at 1100 °C, and the values of $T_{20\%}$ and $T_{90\%}$ increase. But the addition of alkaline earths obviously improves the activity of Pd/Ce–Zr/Al_2O_3 catalyst at lower reaction temperature, and the $T_{20\%}$ decreases in the order: Pd/Ce–Zr/Al_2O_3 (365 °C) > Pd/Ce–Zr–Mg/Al_2O_3 (350 °C) > Pd/Ce–Zr–Sr/Al_2O_3 (340 °C) > Pd/Ce–Zr–Ba/Al_2O_3 (335 °C) > Pd/Ce–Zr–Ca/Al_2O_3 (330 °C). The activity for methane combustion remarkably decreases for all the catalysts after calcined at 1200 °C (see Fig. 5). Interestingly, there is a large difference in the catalytic performance of the catalysts for methane combustion. The $T_{20\%}$ decreases in the order: Pd/Ce–Zr–Ba/Al_2O_3 (550 °C) > Pd/Ce–Zr/Al_2O_3 (525 °C) > Pd/Ce–Zr–Mg/Al_2O_3 (490 °C) > Pd/Ce–Zr–Ca/Al_2O_3 (460 °C) > Pd/Ce–Zr–Sr/Al_2O_3 (400 °C). But when the reaction temperature rises to 625 °C, the methane conversion is 98% for the Pd/Ce–Zr–Ca/Al_2O_3 catalyst, 50% for Pd/Ce–Zr/Al_2O_3 catalyst, and 40% for Pd/Ce–Zr–Ba/Al_2O_3 catalyst, respectively. The results show that the addition of alkaline earths except Ba obviously improves the thermal stability of Pd/Ce–Zr/Al_2O_3 catalyst for methane combustion.

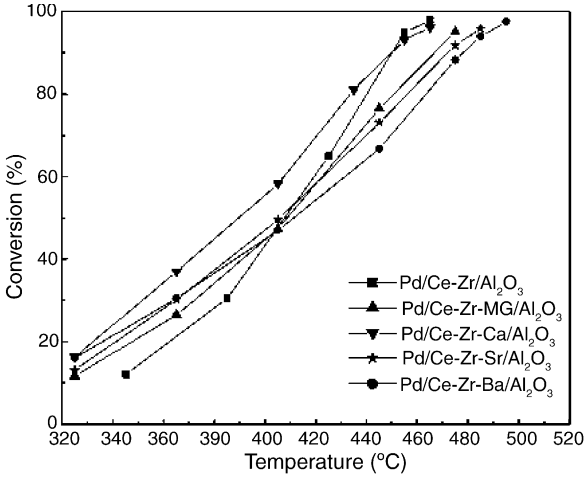

Fig. 4. Light-off curves of methane oxidation over Pd/Ce–Zr/Al_2O_3 and Pd/Ce–Zr–M/Al_2O_3 (M = Mg, Ca, Sr, Ba) catalysts calcined at 1100 °C.

Fig. 6 gives TEM pictures of Pd/Ce–Zr/Al_2O_3, Pd/Ce–Zr–Ca/Al_2O_3 catalysts calcined at 500, 1100 and 1200 °C, respectively. From Fig. 6, it can be seen that the average sizes of Pd particle for Pd/Ce–Zr/Al_2O_3 and Pd/Ce–Zr–Ca/Al_2O_3 calcined at 500 °C are about 10 and 8 nm, respectively, and the sintering of Pd particles and supports occurs obviously after calcined at 1100 or 1200 °C. This is due to the higher pretreatment temperature leading to an obvious decrease in surface area, which causes poor dispersion of palladium. For Pd/Ce–Zr/Al_2O_3 catalyst, the particle size of Pd becomes larger with an average size of about 25 nm after calcined at 1100 °C, and serious sintering and encapsulation phenomena of Pd particles duo to significant agglomeration of support occur after calcined at 1200 °C, with an average particle size of about 41 nm. For the Pd/Ce–Zr–Ca/Al_2O_3 catalyst, the dispersion of Pd particles is obviously improved because of the addition of Ca, and the average size of Pd particle is only about 14 nm after calcined at 1100 °C. The size of Pd particles obviously increases after calcined at 1200 °C, too. But many small Pd particles can still be observed. This indicates that the addition of Ca would inhibit the sintering of Pd particles in Pd/Ce–Zr–Ca/Al_2O_3 catalyst because of increasing the thermal stability of its support, and thus improves the thermal stability of the supported Pd catalyst.

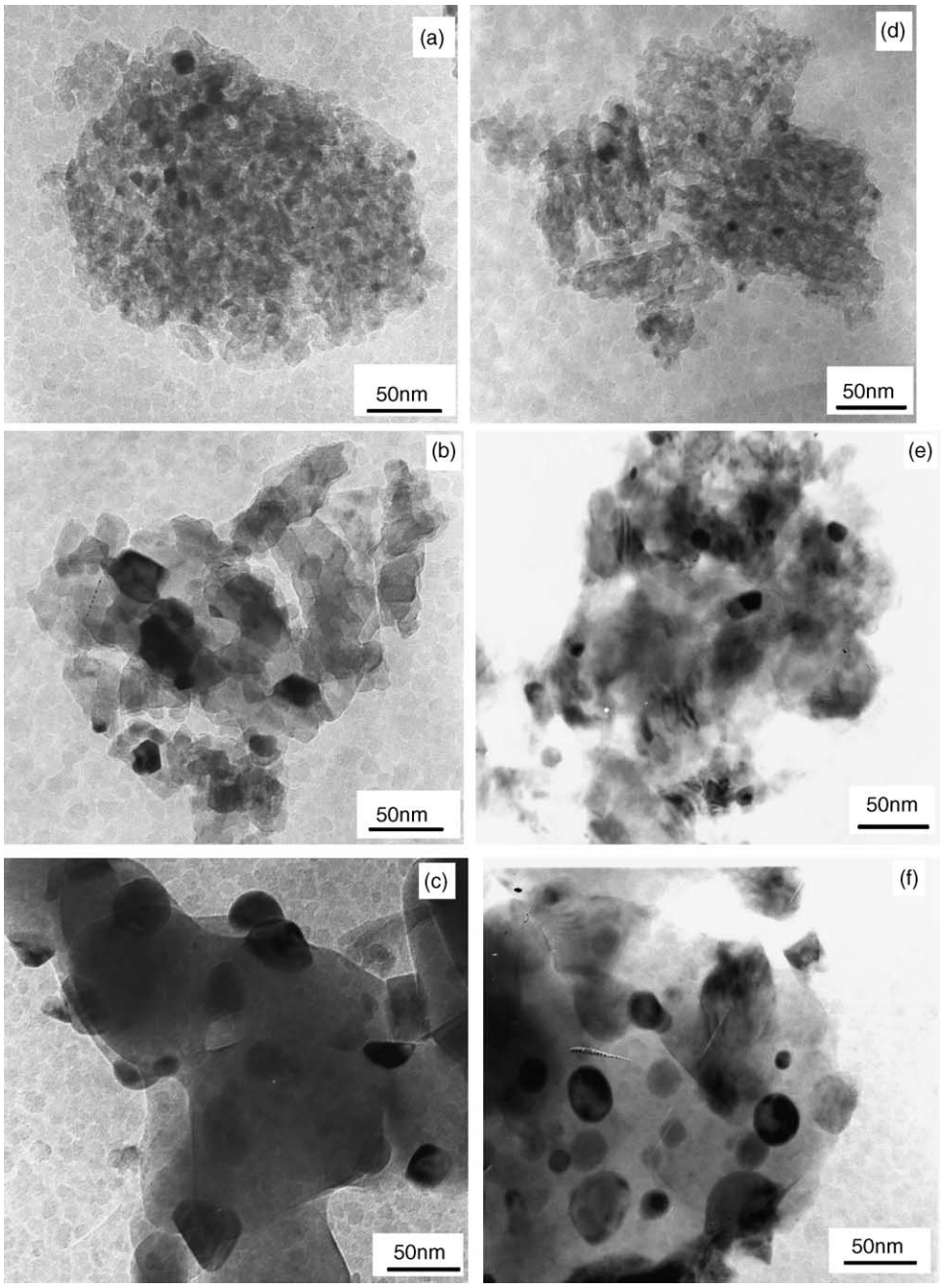

Fig. 6. The TEM photographs of the catalysts: (a) Pd/Ce–Zr/Al_2O_3 calcined at 500 °C; (b) Pd/Ce–Zr/Al_2O_3 calcined at 1100 °C; (c) Pd/Ce–Zr/Al_2O_3 calcined at 1200 °C; (d) Pd/Ce–Zr–Ca/Al_2O_3 calcined at 500 °C; (e) Pd/Ce–Zr–Ca/Al_2O_3 calcined at 1100 °C; (f) Pd/Ce–Zr–Ca/Al_2O_3 calcined at 1200 °C.

3.4. H_2-TPR

The reducibility of supported palladium catalysts is an important factor influencing its catalytic property. H_2-TPR profiles of the Pd/Al_2O_3, Pd/Ce–Zr/Al_2O_3 and Pd/Ce–Zr–M/Al_2O_3 catalysts calcined at 500 °C are shown in Fig. 7 and values of the H_2 consumption and peak temperature maxima are shown in Table 2. From Fig. 7 and Table 2, it can be seen that palladium oxide supported on Al_2O_3 is more easily reduced and TPR profile of Pd/Al_2O_3 exhibits one hydrogen consumption peak at 10 °C representing the reduction of PdO species finely dispersed on Al_2O_3 and a negative peak at 90 °C generally attributed to the decompositon of palladium hydride [24], while H_2-TPR profile of Pd/Ce–Zr/Al_2O_3 catalyst exhibits three hydrogen consumption peaks at 35 °C (α peak), 45 °C (β peak), 102 °C (γ peak) and a negative peak at about 90 °C. The positive peaks are attributed to the reduction of PdO species, which indicates variation in the distribution of PdO with support composition. According to the previous work in our research group, the reduction of PdO species appears at 60–90 °C for Pd/Ce–Zr–O catalysts [25,26]. So we suggest that α peak may be the PdO dispersed on

Table 2
H_2 consumption and temperature of TPR peaks for the catalysts calcined at 500 °C

Catalysts	α Peak		β Peak		γ Peak	
	H_2 consumption ($\mu mol/g_{cat}$)	Peak temperature (°C)	H_2 consumption ($\mu mol/g_{cat}$)	Peak temperature (°C)	H_2 consumption ($\mu mol/g_{cat}$)	Peak temperature (°C)
Pd/Al_2O_3	46.1 ± 0.88	11				
$Pd/Ce–Zr/Al_2O_3$	24.5 ± 0.49	35	13.5 ± 0.31	45	8.5 ± 0.22	102
$Pd/Ce–Zr–Mg/Al_2O_3$	17.1 ± 0.37	18	13.8 ± 0.35	44	14.9 ± 0.37	97
$Pd/Ce–Zr–Ca/Al_2O_3$	38.5 ± 0.76	17	–	–	14.6 ± 0.36	101
$Pd/Ce–Zr–Sr/Al_2O_3$	17.5 ± 0.38	18	14.9 ± 0.36	48	15 ± 0.37	101
$Pd/Ce–Zr–Ba/Al_2O_3$	17.9 ± 0.39	18	15.3 ± 0.37	40	14.8 ± 0.37	100

alumina-rich grains and the β peak may be the PdO dispersed on Ce–Zr-rich grains. There have been analogy reports in the H_2-TPR profiles of $Pd/TiO_2–Al_2O_3$ catalysts by Wang [27]. For the γ peak, it is suggested that the stable PdO species are present on the $Ce–Zr/Al_2O_3$ support due to the interaction of Pd and ZrO_2 [28,29]. In addition, we can see that the α peak shifts to lower temperature about decreasing 17 °C after the addition of alkaline earths, indicating that the addition of alkaline earths increases the reducibility of PdO dispersed on alumina-rich grains. The steep feature of TPR patterns implies PdO be reduced through a self-catalyzing mechanism [30]. Addition of alkaline earths to the supported Pd catalysts could lead to a change in the net charge density at the metal, which could result in an enhancement in hydrogen adsorption and hydrogenation activity of the catalysts [31,32]. In addition, the presence of alkaline earths on the support surface improves the dispersion of PdO species. So the PdO could be reduced at lower temperature after the addition of alkaline earths. From the results of Fig. 3 and our previous studies (the $T_{20\%}$ for Pd/Al_2O_3 catalyst is 321 °C), we find that the trend of the α peak temperature decreasing after the addition of rare earths is similar to that of their oxidation activities increasing under lower reaction temperature conditions. This suggests that the catalytic activity may be related to the reducibility of PdO species finely dispersed on alumina-rich grains, and the higher the reducibility of the PdO species, the higher the catalytic activities under lower reaction temperature conditions. This phenomenon also demonstrates that the reduction step is the rate-determining step in methane combustion reaction catalyzed by supported PdO [18].

H_2-TPR profiles of $Pd/Ce–Zr/Al_2O_3$, $Pd/Ce–Zr–Ca/Al_2O_3$ and $Pd/Ce–Zr–Ba/Al_2O_3$ catalysts calcined at 1100 °C and 1200 °C are shown in Figs. 8 and 9, respectively. For the catalysts calcined at 1100 °C (see Fig. 8), the hydrogen consumption peak and hydrogen desorption peak in all catalysts become obviously sharper, indicating that the sintering phenomena of PdO species occurs after calcined at 1100 °C. H_2-TPR profiles of the catalysts calcined at 1200 °C show evident distinctness as compared with the catalysts cal-

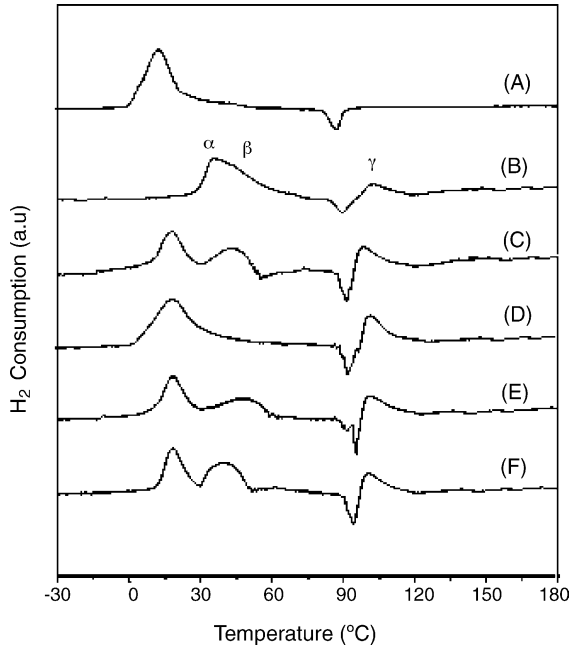

Fig. 7. TPR profiles of the catalysts calcined at 500 °C: (A) Pd/Al_2O_3; (B) $Pd/Ce–Zr/Al_2O_3$; (C) $Pd/Ce–Zr–Mg/Al_2O_3$; (D) $Pd/Ce–Zr–Ca/Al_2O_3$; (E) $Pd/Ce–Zr–Sr/Al_2O_3$; (F) $Pd/Ce–Zr–Ba/Al_2O_3$.

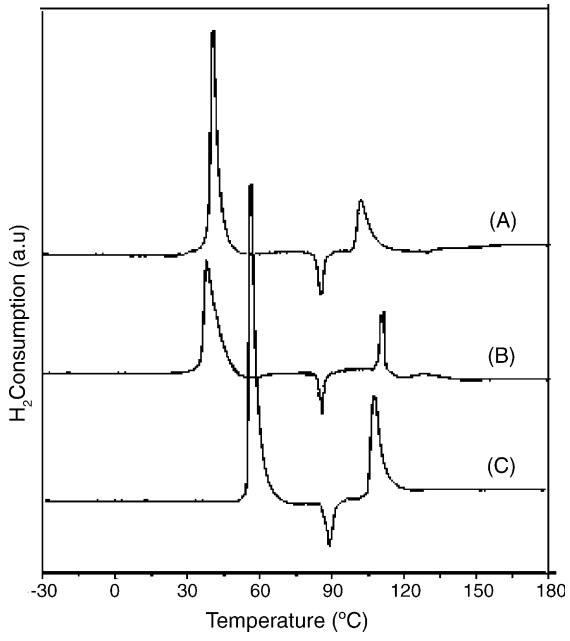

Fig. 8. TPR profiles of the catalysts calcined at 1100 °C: (A) $Pd/Ce–Zr/Al_2O_3$; (B) $Pd/Ce–Zr–Ca/Al_2O_3$; (C) $Pd/Ce–Zr–Ba/Al_2O_3$.

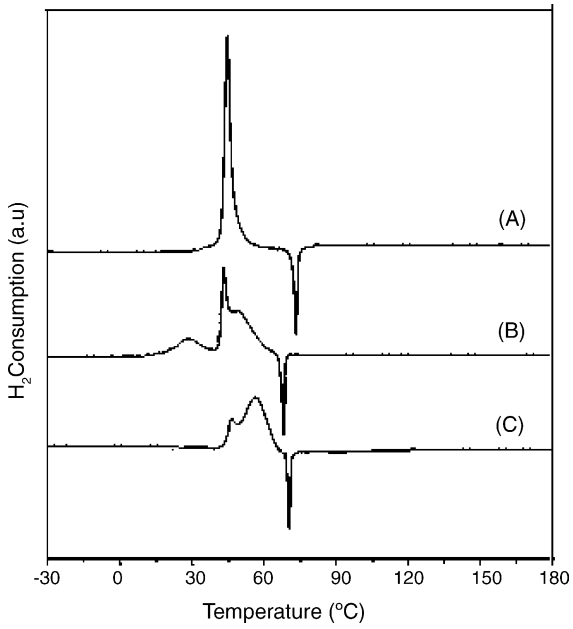

Fig. 9. TPR profiles of the catalysts calcined at 1200 °C: (A) $Pd/Ce–Zr/Al_2O_3$; (B) $Pd/Ce–Zr–Ca/Al_2O_3$; (C) $Pd/Ce–Zr–Ba/Al_2O_3$.

cined at <1200 °C (see Fig. 9). The negative peak shifts to lower temperature, while the hydrogen consumption peak at above100 °C disappears and the shape of hydrogen consumption peak in the range of 10–70 °C is different from each other. The changes of the TPR profiles may be due to phase transformation of alumina support. The XRD results show that the crystalline structure of alumina converts to α-alumina phase after calcinations at 1200 °C. So the phase transformation of alumina causes a drastic decrease of the surface area, which results in significant change of the distribution of PdO on the supports. For the $Pd/Ce–Zr/Al_2O_3$ catalyst calcined at 1200 °C, the phenomenon of particle of palladium encapsulation occurs. For all the catalysts γ peak disappears, which suggests that PdO species on the surface of $Ce–Zr/Al_2O_3$ or $Ce–Zr–M/Al_2O_3$ supports could be migrated and decomposed into metallic Pd due to weakening the interaction of PdO and Ce–Zr oxides or ZrO_2 at high temperature of 1200 °C [29]. A part of PdO species dispersed on Ce–Zr-rich grains and had strong interaction with ZrO_2 may be migrated on alumina-rich grains. The reduction temperature of PdO species in the catalysts decreases in the order: $Pd/Ce–Zr–Ba/Al_2O_3$ > $Pd/Ce–Zr/Al_2O_3$>$Pd/Ce–Zr–Ca/Al_2O_3$. This order is also in accordance with that of their oxidation activities increasing.

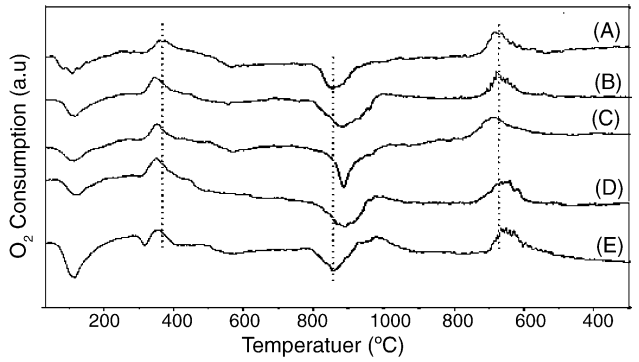

Fig. 10. TPO profiles of the catalysts calcined at 500 °C: (A) $Pd/Ce–Zr/Al_2O_3$; (B) $Pd/Ce–Zr–Mg/Al_2O_3$; (C) $Pd/Ce–Zr–Ca/Al_2O_3$; (D) $Pd/Ce–Zr–Sr/Al_2O_3$; (E) $Pd/Ce–Zr–Ba/Al_2O_3$.

3.5. O_2-TPO and CH_4/O_2-TPSR

Fig. 10 shows the results of TPO experiment over the $Pd/Ce–Zr/Al_2O_3$ and $Pd/Ce–Zr–M/Al_2O_3$ catalysts calcined at 500 °C and values of the O_2 consumption and peak temperature maxima are shown in Table 3. From Fig. 10 and Table 3, it can be seen that TPO profiles of all catalysts show two negative peaks (named as first and third peaks, respectively) representing oxygen desorption and one positive peak (named as second peak) representing oxygen consumption in the range of 30–1000 °C during raising the temperature and one positive peak (named as fourth peak) representing oxygen consumption during lowering the temperature. We suggest that the negative peaks at about 100 and 850 °C are attributed to desorption of adsorption oxygen species and the decomposition of PdO species, respectively, while the positive peaks are attributed to the reoxidation of metallic Pd species during raising/lowering the temperature. However, no oxygen consumption peak is observed in the range of 30–300 °C and the area of PdO decomposition peak is obviously larger than that of oxygen consumption peak at 350 °C, while the amount of H_2 consumption of γ peak (Fig. 7) is almost double of that of O_2 consumption of second peak. The results show that Pd species finely dispersed on alumina-rich grains and Ce–Zr-rich grain corresponding α and β reduction peaks in Fig. 7 have been oxidized at the balance of TPO beginning, and the

Table 3
O_2 consumption and temperature of TPO peaks for the catalysts calcined at 500 °C

Catalysts	Second peak		Third peak		Fourth peak	
	O_2 consumption ($\mu mol/g_{cat}$)	Peak temperature (°C)	O_2 consumption ($\mu mol/g_{cat}$)	Peak temperature (°C)	O_2 consumption ($\mu mol/g_{cat}$)	Peak temperature (°C)
$Pd/Ce–Zr/Al_2O_3$	4.6 ± 0.16	355	−22.1 ± 0.33	860	15.9 ± 0.31	675
$Pd/Ce–Zr–Mg/Al_2O_3$	7.6 ± 0.25	350	−23.1 ± 0.32	880	16.2 ± 0.33	675
$Pd/Ce–Zr–Ca/Al_2O_3$	7.4 ± 0.26	350	−23 ± 0.32	885	17.8 ± 0.39	700
$Pd/Ce–Zr–Sr/Al_2O_3$	7.8 ± 0.27	350	−23.2 ± 0.32	885	16.4 ± 0.32	670
$Pd/Ce–Zr–Ba/Al_2O_3$	7.5 ± 0.24	355	−22.8 ± 0.34	860	16.1 ± 0.35	670

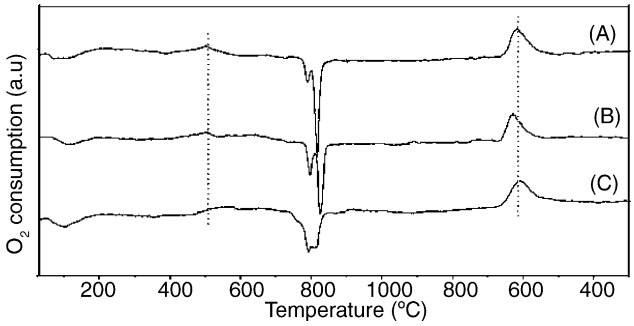

Fig. 11. TPO profiles of the catalysts calcined at 1100 °C: (A) Pd/Ce–Zr/Al_2O_3; (B) Pd/Ce–Zr–Ca/Al_2O_3; (C) Pd/Ce–Zr–Ba/Al_2O_3.

oxygen consumption peak at 350 °C may be attributed to the reoxidation of stable metallic Pd species obtained in the TPR profiles (γ peak). In addition, we can see that the PdO decomposition peak shifts to higher temperature after the addition of alkaline earths except the addition of Ba, indicating that the presence of Mg, Ca, Sr improves the thermal stability of PdO. But the addition of different alkaline earths has different influence on the reoxidation properties of metallic Pd. The reoxidation property of metallic Pd is obviously improved in presence of Ca and its reoxidation temperature shifts to higher temperature than the corresponding temperature observed on Pd/Ce–Zr/Al_2O_3 catalyst.

Figs. 11 and 12 show TPO profiles of the Pd/Ce–Zr/Al_2O_3, Pd/Ce–Zr–Ca/Al_2O_3 and Pd/Ce–Zr–Ba/Al_2O_3 catalysts calcined at 1100 and 1200 °C, respectively. From Fig. 11, it can be seen that after calcined at 1100 °C, areas of oxygen desorption peak at about 100 °C and oxygen consumption peak at about 350 °C decrease obviously and the latter shifts to higher temperature (about 500 °C). In addition, TPO profiles of all catalysts show two peaks of PdO decomposition with maximum at about 780 and 820 °C, and the temperatures of PdO decomposition and its reoxidation during raising and lowering the temperature shift to lower temperature after calcined at 1100 °C, indicating that PdO species are more easily decomposed and the ability of its reoxidation decreases duo to the weakening of the interaction of Pd species and

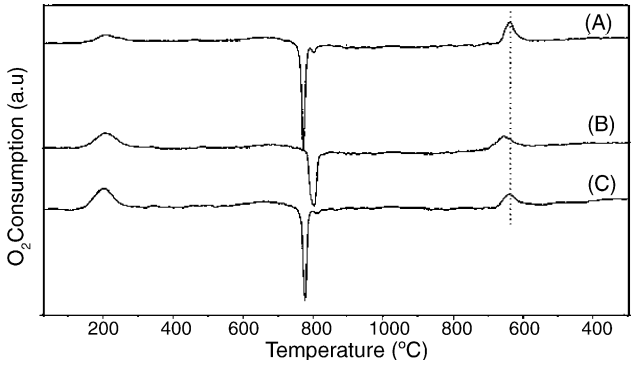

Fig. 12. TPO profiles of the catalysts calcined at 1200 °C: (A) Pd/Ce–Zr/Al_2O_3; (B) Pd/Ce–Zr–Ca/Al_2O_3; (C) Pd/Ce–Zr–Ba/Al_2O_3.

support. But the presence of Ca in Pd/Ce–Zr/Al_2O_3 would obviously improve the thermal stability of PdO and the ability of its reoxidation. For the catalysts calcined at 1200 °C (see Fig. 12), the oxygen desorption peak at about 100 °C and the oxygen consumption peak at 500 °C disappear and a positive peak representing oxygen consumption at about 200 °C appears. This suggests that the oxidation of large particle size of metallic Pd species becomes difficult due to the decreasing of the ability of adsorbing oxygen. In addition, the decomposition peak of PdO occurs obviously change too. Relative intensity of the two decomposition peaks takes place great change compared with that of the catalysts calcined at 1100 °C. For the Pd/Ce–Zr–Ca/Al_2O_3 and Pd/Ce–Zr–Ba/Al_2O_3 catalysts, the decomposition of PdO takes place with maximum at 800 and 775 °C, respectively. The addition of Ca obviously increases the temperatures of PdO decomposition and its reoxidation. The above results just prove the variation of catalytic activity for the catalysts calcined at 1100 or 1200 °C.

In order to investigate the relation of methane combustion activity with properties of PdO decomposition and its reoxidation, CH_4/O_2-TPSR experiments of the Pd/Ce–Zr/Al_2O_3 and Pd/Ce–Zr–Ca/Al_2O_3 catalysts calcined at 1100 °C are carried out (see Fig. 13). The results show that the presence of Ca in Pd/Ce–Zr/Al_2O_3 obviously decreases the beginning temperature of methane combustion. However, it is interesting that there is a trend of CH_4 oxidation activity decreasing in the range of 750–900 °C during raising the temperature and in the range of 850–660 °C during lowering the temperature, in particular, there is no catalytic activity for CH_4 combustion in the range of 750–660 °C. Comparing the TPSR profile with the TPO of the Pd/Ce–Zr/Al_2O_3 catalyst, it may be seen that the activity decrease in the heating process is related with the decomposition of PdO into the less active Pd. A strong

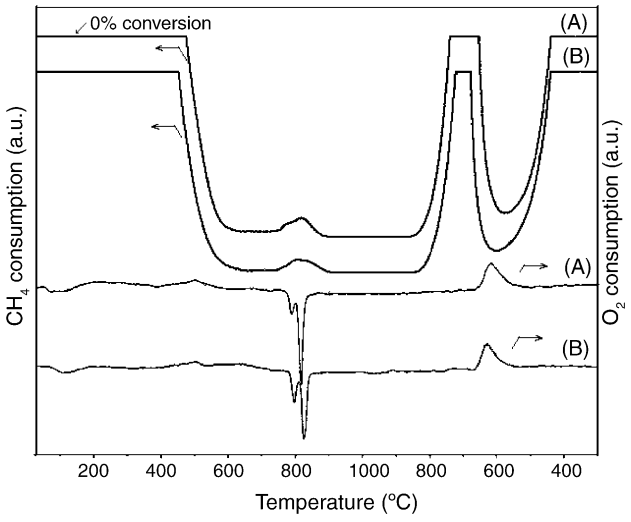

Fig. 13. Comparison between the CH_4 profiles measured in a TPSR experiment and the O_2 profiles measured in a TPO experiment: (A) Pd/Ce–Zr/Al_2O_3; (B) Pd/Ce–Zr–Ca/Al_2O_3.

drop of activity during the cooling-down step is due to that Pd is still at the metallic state, and the activity increases until PdO reforms. At the same time, the presence of Ca improves thermal stability of PdO and reoxidation property of Pd, thus increasing their activities of methane oxidation and thermal stability of catalyst.

4. Conclusions

The effects of alkaline earths (Mg, Ca, Sr, Ba) on the catalytic activity of Pd/Ce–Zr/Al_2O_3 for methane combustion are investigated. The catalysts are characterized using BET, XRD, TEM, H_2-TPR, O_2-TPO and CH_4/O_2-TPSR measurements. Activity tests in methane combustion show that the addition of trace alkaline earths to Pd/Ce–Zr/Al_2O_3 catalyst obviously increases the catalytic activity of the catalysts under lower reaction temperature conditions, and Pd/Ce–Zr–Ca/Al_2O_3 exhibits the highest catalytic activity and thermal stability among all catalysts. The results of H_2-TPR show that Pd/Ce–Zr/Al_2O_3 catalyst exhibits three hydrogen consumption peaks attributed to the reduction of PdO species dispersed on alumina-rich grains and on Ce–Zr-rich grains and stable PdO species due to the interaction of Pd and ZrO_2 and one hydrogen desorption peak generally attributed to the decompositon of palladium hydride. The addition of alkaline earths increases the reducibility of PdO dispersed on alumina-rich grains. The results of O_2-TPO show that two oxygen desorption peaks attributed to desorption of adsorption oxygen species and the decomposition of PdO species in the range of 30–1000 °C during raising the temperature, respectively, and one oxygen consumption peak attributed to the reoxidation of metallic Pd species in the range of 1000–300 °C during lowering the temperature. The addition of alkaline earths, in particular, Ca, to Pd/Ce–Zr/Al_2O_3 catalyst inhibits the site growth and decomposition of PdO particles and improves the reduction–reoxidation properties of the active PdO species, which increases the catalytic activity and thermal stability of the Pd/Ce–Zr/Al_2O_3 catalyst.

Acknowledgements

We gratefully acknowledge the financial supports from the Ministry of Science and Technology of China (No. 2004 CB 719504) and Nature Science Foundation of Zhejiang Province (No. Z504032).

References

[1] H. Arai, M. Machida, Appl. Catal. A 138 (1996) 161.
[2] D.L. Trimm, Appl. Catal. 7 (1983) 249.
[3] R. Prasad, L.A. Kennedy, E. Ruckentein, Catal. Rev. 26 (1984) 1.
[4] P. Forzatti, G. Groppi, Catal. Today 54 (1999) 165.
[5] G. Pecchi, P. Reyes, R. Gomez, T. Lopez, J.L.G. Fierro, Appl. Catal. B 17 (1998) 7.
[6] L.D. Pfefferle, W.C. Pfefferle, Catal. Rev. 29 (1987) 219.
[7] K. Eguchi, H. Arai, Catal. Today 29 (1996) 379.
[8] L.F. Liotta, G. Deganello, J. Mol. Catal. 204–205 (2003) 763.
[9] B.W.-L. Jang, R.M. Nelson, J.J. Spivey, M. Ocal, R. Oukaci, G. Marcelin, Catal. Today 47 (1999) 103.
[10] S. Suhonen, M. Valden, M. Hietikko, R. Laitinen, A. Savimäki, M. Härkönen, Appl. Catal. A 218 (2001) 151.
[11] K.-i. Muto, N. Kadata, M. Niwa, Catal. Today 35 (1997) 145.
[12] R. Burch, F.J. Urbano, Appl. Catal. A 124 (1995) 121.
[13] P. Reyes, A. Figueroa, G. Pecchi, J.L.G. Fierro, Catal. Today 62 (2000) 209.
[14] T.J. Toops, A.B. Walters, M.A. Vannice, Appl. Catal. A 233 (2002) 125.
[15] B. Kucharczyk, W. Tylus, L. Kepinski, Appl. Catal. B 49 (2004) 27.
[16] K. Persson, P.O. Thevenin, K. Jansson, J. Agrell, S.G. Järås, L.J. Pettersson, Appl. Catal. A 249 (2003) 165.
[17] S. Suhonen, M. Valden, M. Pessa, A. Savimäki, M. Härkönen, M. Hietikko, J. Pursiainen, R. Laitinen, Appl. Catal. A 207 (2001) 113.
[18] L.-f. Yang, C.-k. Shi, X.-e. He, J.-x. Cai, Appl. Catal. B 38 (2002) 117.
[19] K. Narui, H. Yata, K. Furuta, A. Nishida, Y. Kohtoku, T. Matsuzaki, Appl. Catal. A 179 (1995) 165.
[20] M.A. Fraga, E.S. d. Souza, F. Villain, L.G. Appel, Appl. Catal. A 259 (2004) 57.
[21] J. Kašpar, P. Fornasiero, M. Graziani, Catal. Today 50 (1999) 285.
[22] P.O. Thevenin, A. Alcalde, L.J. Pettersson, S.G. Järås, J.L.G. Fierro, J. Catal. 215 (2003) 78.
[23] R.D. Monte, P. Fornasiero, J. Kašpar, P. Rumori, G. Gubitosa, M. Graziani, Appl. Catal. B 24 (2000) 157.
[24] G. Chen, W.T. Chou, C.T. Yeh, Appl. Catal. 8 (1983) 389.
[25] M.-F. Luo, X.-M. Zheng, Appl. Catal. A 189 (1999) 15.
[26] L. Ma, M.-F. Luo, L.-F. Han, S.-Y. Chen, React. Kinet. Catal. Lett. 70 (2002) 357.
[27] C.-B. Wang, H.-K. Lin, C.-M. Ho, J. Mol. Catal. 180 (2002) 285.
[28] K. Asakura, Y. Iwasawa, J. Phys. Chem. 96 (1992) 7386.
[29] K. Narui, K. Furuta, H. Yata, A. Nishida, Y. Kohtoku, T. Matsuzaki, Catal. Today 45 (1998) 173.
[30] N.W. Hurst, S.J. Gentry, A. Jones, B.D. McNicol, Catal. Rev. Sci. Eng. 24 (1982) 233.
[31] U.R. Pillai, E. Sahle-Demessie, Appl. Catal. A 281 (2005) 31.
[32] S. Scirè, S. Minicò, C. Crisafulli, Appl. Catal. A 235 (2002) 21.